# Stability of Intramolecular DNA Quadruplexes: Comparison with DNA Duplexes†

Antonina Risitano and Keith R. Fox*

*Division of Biochemistry and Molecular Biology, School of Biological Sciences, University of Southampton, Bassett Crescent East, Southampton SO16 7PX, U.K.*

*Received October 14, 2002; Revised Manuscript Received April 4, 2003*

ABSTRACT: We have determined the stability of intramolecular quadruplexes that are formed by a variety of G-rich sequences, using oligonucleotides containing appropriately placed fluorophores and quenchers. The stability of these quadruplexes is compared with that of the DNA duplexes that are formed on addition of complementary C-rich oligonucleotides. We find that the linkers joining the G-tracts are not essential for folding and can be replaced with nonnucleosidic moieties, though their sequence composition profoundly affects quadruplex stability. Although the human telomere repeat sequence d[$G_3(TTAG_3)_3$] folds into a quadruplex structure, this forms a duplex in the presence of the complementary C-rich strand at physiological conditions. The *Tetrahymena* sequence d[$G_4(T_2G_4)_3$], the sequence d[$G_3(T_2G_3)_3$], and sequences related to regions of the *c-myc* promoter d($G_4AG_4T)_2$ and d($G_4AG_3T)_2$ preferentially adopt the quadruplex form in potassium-containing buffers, even in the presence of a 50-fold excess of their complementary C-rich strands, though the duplex predominates in the presence of sodium. The HIV integrase inhibitor d[$G_3(TG_3)_3$] forms an extremely stable quadruplex which is not affected by addition of a 50-fold excess of the complementary C-rich strand in both potassium- and sodium-containing buffers. Replacing the TTA loops of the human telomeric repeat with AAA causes a large decrease in quadruplex stability, though a sequence with AAA in the first loop and TTT in the second and third loops is slightly more stable.

Guanine-rich nucleic acid sequences can fold into four-stranded DNA structures that contain stacks of G-quartets (Figure 1A) (*1*−*4*). These quadruplexes (tetraplexes) can be formed by the intermolecular association of four DNA molecules (*5*, *6*), dimerization of sequences that contain two G-tracts (*7*−*9*), or by the intramolecular folding of a single strand containing four blocks of guanines (*10*−*17*). The formation of these stable complexes depends on the presence of monovalent cations (*18*−*21*). Sodium and potassium promote stable folding while it is inhibited by lithium (*22*). The cations are coordinated by the guanine carbonyls and may lie between or within the plane of each quartet. Sodium and potassium may promote the formation of different complexes, on account of their different sizes, their hydration energies (*23*), and their interaction with residues in the loops (*24*). In general, the most stable complexes are formed in the presence of potassium.

These structures have recently received considerable attention as G-rich sequences are found in a number of important DNA regions. In particular, telomeres contain highly repeated G-rich sequences which consist of $(GGGTTA)_n$ in humans and most other higher eukaryotes, $(GGGGTT)_n$ in *Tetrahymena* and $(GGGGTTTT)_n$ in *Oxytricha*. G-rich sequences with the potential to form quadruplexes are also found in other locations including the *c-myc* promoter (*25*, *26*), the immunoglobulin switch region (*27*), and insulin regulatory sequences (*28*). Several aptamers are also based on G-quadruplex structures including the thrombin-binding aptamer (TBA, GGTTGGTGTGGTTGG) (*17*, *29*) and an inhibitor of HIV integrase (T30695, GGGTGGGTGGGTGGGT) (*15*, *16*, *24*).

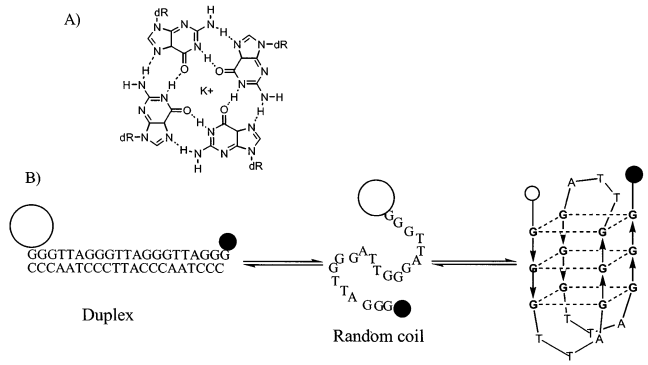


FIGURE 1: (A) Chemical structure of the G-quartet. (B) Schematic representation of the folding of the intramolecular quadruplexes and the formation of duplexes with the complementary oligonucleotide. The fluorophore and quencher are represented by the open and closed circles, respectively. The duplex is shown on the left, the random coil is in the center, and the folded quadruplex is shown on the right. Although several different folded structures are possible, for simplicity only one antiparallel structure is shown.

Small changes in the sequences of these complexes can have profound effects on their folding and may affect their thermodynamic stability. The human and *Oxytricha* telomeric sequences consist of stacks of three and four G-quartets, respectively, with TTA or TTTT in the connecting loops (*10*, *12*, *13*). The HIV integrase inhibitor T30695 consists of two stacked G-quartets with two bases (TG) in each of the loops (*15*, *16*, *24*). In contrast, the *Tetrahymena* sequence, which differs from the human sequence by exchanging A for G in each repeat and which could in principle generate four

† This work was supported by a grant from the European Union.

* Corresponding author: tel, +44 23 8059 4374; fax, +44 23 8059 4459; e-mail, K.R.Fox@soton.ac.uk.

10.1021/bi026997v CCC: $25.00 
Published on Web 05/08/2003

stacked G-quartets linked by two-base loops, folds to form only three quartets with variable loops containing TGGT, TTG, and TT (*11*). Other quadruplexes, such as that formed by the *c-myc* sequence, can adopt complex structures that contain several contiguous G-residues in the loops (*25*). The orientation of the strands is all-parallel for intermolecular complexes (*5*, *6*) but can be alternating antiparallel (*10*, *12*), parallel (*13*), or three parallel with one antiparallel (*11*) for the intermolecular complexes. In these structures the central loop can be either crossed or uncrossed.

Once formed, these complexes are extremely stable and dissociate very slowly (much more slowly than duplexes) (*30*−*32*). However, within the cell most G-rich sequences will be present along with their complementary C-rich strands, which will generate competing duplex structures. The formation of quadruplex or duplex structures will therefore depend on the relative stability of the quadruplex and duplexes. There have previously been a few studies on the competition between duplex and quadruplex structures (*33*, *34*) and the effects of quadruplex-binding ligands on this equilibrium (*26*). These have shown that, under physiological conditions, the human quadruplex sequence is predominantly in the duplex conformation.

In this paper we have examined the melting and annealing profiles of several G-rich sequences and compared their stability with the Watson−Crick duplexes formed with the complementary C-rich strands. For this we have used oligonucleotides that contain appropriately placed fluorophores (fluorescein) and quenchers (methyl red) as previously described (*35*). The basis of these experiments is illustrated in Figure 1B. When the oligonucleotide folds into an intramolecular quadruplex, the fluorophore and quencher are in close proximity and the fluorescence is quenched. When this melts into the random-coil form, the fluorophore and quencher are no longer in close proximity and there is a large increase in fluorescence. On addition of the complementary (C-rich) oligonucleotide there will be competition between the quadruplex and duplex structures in which the duplex will have a high fluorescence as the fluorophore and quencher are separated by a large distance.

## MATERIALS AND METHODS

*Oligonucleotides*. Oligonucleotides containing fluorophores and quenchers were synthesized on an Applied Biosystems 394 DNA/RNA synthesizer on either the 0.2 or 1 $\mu$mol scale and were purchased from Oswel DNA service (Southampton, U.K.). These were purified by HPLC or on denaturing polyacrylamide gels. Methyl red and fluorescein were incorporated into the oligonucleotides using MeRed-dR or Fam-dR (*35*). Unmodified oligonucleotides were also purchased from Oswel DNA service. The sequences of the oligonucleotides used in these studies are shown in Table 1.

*Buffers*. Oligonucleotides were diluted to 0.25 $\mu$M in sodium phosphate, pH 7.4, or potassium phosphate, pH 7.4, at buffer concentrations of 1−100 mM.

*Fluorescence Melting*. Fluorescence melting curves were determined in a Roche LightCycler, as previously described (*35*) in a total reaction volume of 20 $\mu$L. For each reaction the oligonucleotide was diluted to a final concentration of 0.25 $\mu$M in the appropriate buffer. In a typical experiment the oligonucleotides were first denatured by heating to 95 °C for 5 min. They were then annealed by cooling to 30 °C at a rate of 0.1 deg·s $^{-1}$ (the slowest heating and cooling rate for the LightCycler). The samples were maintained at 30 °C for 5 min before being slowly heated to 95 °C (0.1 deg·s$^{-1}$). Recordings were taken during both the annealing and melting steps. The LightCycler has one excitation source (488 nm), and the changes in fluorescence were measured at 520 nm. In these experiments we assume that addition of the fluorescent moieties does not significantly affect quadruplex stability. Although the quadruplex structures reported in this work have slightly higher $T_m$ values than some of the published values (*34*) (albeit in different buffer systems), any effects of the fluorophores will be constant for all of the oligonucleotides studied and should not affect their relative stabilities.

Table 1: Sequences of the Fluorescently Labeled Oligonucleotides Used in This Work

| oligo name | fluorophore/quencher oligonucleotide[a] |
|---|---|
| G3TTA | Q-TGGGTTAGGGTTAGGGTTAGGG-F |
| G3H2 | Q-TGGGHHGGGHHGGGHHGGG-F |
| G3AT | F-GGGAAAGGGTTTGGGTTTGGG-Q |
| G3T | F-GGGTGGGTGGGTGGG-Q |
| G3T2 | F-GGGTTGGGTTGGGTTGGG-Q |
| G4T2 | F-GGGGTTGGGGTTGGGGTTGGGG-Q |
| G3A3 | F-GGGAAAGGGAAAGGGAAAGGG-Q |
| myc-1 | F-GGGGAGGGGTGGGGAGGGG-Q |
| myc-2 | F-GGGGAGGGTGGGGAGGG-Q |

[a] Abbreviations: F = dR-FAM, Q = dR-MeRed, and H = hexaethylene glycol.

*Data Analysis*. $T_m$ and $\Delta H$ values for the quadruplexes were determined from van't Hoff analysis of the melting profiles using FigP for Windows. This analysis assumes a simple two-state equilibrium between the folded and unfolded forms. In some instances the melting curves showed a linear change in fluorescence with temperature in regions outside the melting transition. This was accounted for by fitting a straight line to the first and last portions of the fluorescence curve. All reactions were performed at least twice, and the calculated $T_m$ values usually differed by <0.5 K with a 5% variation in $\Delta H$. As described below, we observed hysteresis between the melting and annealing curves in the presence of low concentrations of potassium. This occurs when the reaction is not at thermodynamic equilibrium and complicates the thermodynamic analysis. As a result the calculated $\Delta H$ values may not be strictly accurate in the presence of potassium, and these are therefore presented as $\Delta H_{app}$. For the reasons discussed below, the $T_m$ and $\Delta H$ values were obtained from analysis of the annealing rather than the melting transitions.

## RESULTS

Our previous work with the human telomeric sequence G3TTA showed that there was little hysteresis between the annealing and melting curves when the reaction was performed in 50 mM potassium phosphate, pH 7.4 (*35*). However, we compared the annealing and melting profiles for all of the oligonucleotides used in this work, and representative curves for oligonucleotides G3TTA and G3H2 are shown in Figure 2. There is little or no hysteresis (<2 K) when the experiments are performed in sodium-containing buffers (not shown). However, it can be seen that there is

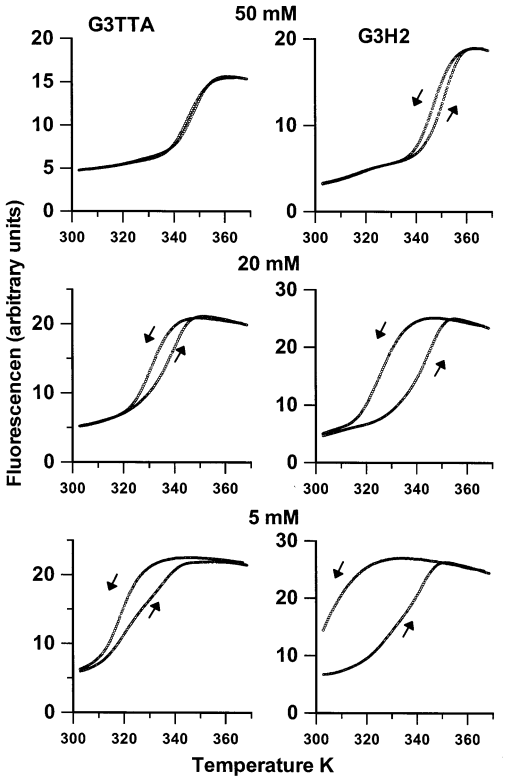


FIGURE 2: Fluorescence melting and annealing curves for oligonucleotides G3TTA (left-hand panels) and G3H2 (right-hand panels) in 50, 20, and 5 mM potassium phosphate buffer. The *y*-axis shows the fluorescence (arbitrary units). The arrows show the direction of the temperature change.

significant hysteresis in low concentrations of potassium. Although the annealing and melting curves are very similar in 50 mM potassium, there are clear differences at lower ionic strengths, and the $T_m$ for the annealing curves is always lower than that for the melting curves. This effect was seen with all of the oligonucleotides shown in Table 1 and was most pronounced for G3H2. This hysteresis occurs because the heating and cooling curves are not in thermodynamic equilibrium; i.e., the temperature change is faster than the rate at which the reactions relax to a new equilibrium. Such hysteresis could reflect either a slow rate of association (which would depress the apparent annealing $T_m$) or a slow rate of dissociation (which would elevate the apparent $T_m$ for the melting reaction). Since these were all intramolecular reactions, the rate of association is unlikely to be slow, whereas the rate of quadruplex dissociation (of intermolecular quadruplexes) is known to be very slow (*30*−*32*). We confirmed this difference in the rates of association and dissociation for oligonucleotides G3TTA and G3H2 by performing simple temperature-jump experiments with the LightCycler. Previous studies have shown that increasing the rate of temperature change affects the melting transitions but has little effect on the annealing curves (*35*). Furthermore, it can be seen that, although the annealing curves are the expected sigmoidal shape, the melting curves at low ionic strengths (Figure 2) show unusual or biphasic transitions. For these reasons we consider that the annealing profiles are a better indication of the situation at thermodynamic equilibrium than the melting curves. We have therefore analyzed the annealing rather than the melting transitions in all the experiments described below. It should be noted that these

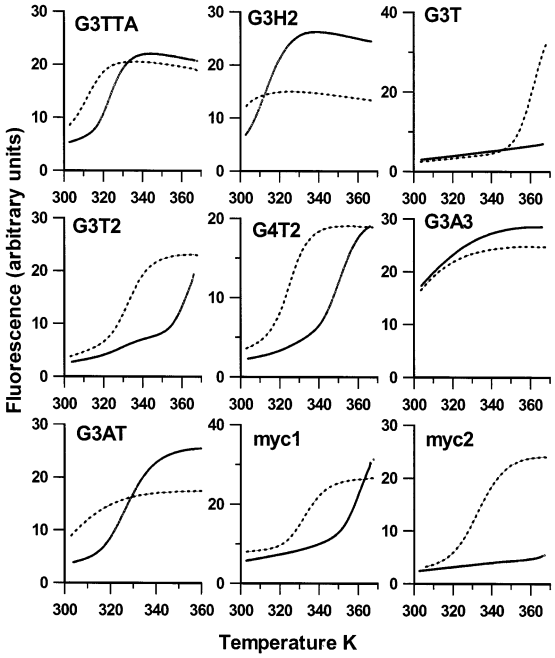


FIGURE 3: Representative fluorescence annealing curves for all of the oligonucleotides used in this work. These curves were obtained in 10 mM potassium phosphate, pH 7.4 (solid lines), or 10 mM sodium phosphate, pH 7.4 (dashed lines).

nonequilibrium conditions may introduce some errors into the $\Delta H$ values estimated in the presence of low concentrations of potassium, and these are reported as $\Delta H_{app}$.

*Inter- or Intramolecular Complexes?* Although the oligonucleotides used in this work were designed to form intramolecular quadruplexes, it is essential to demonstrate that they are not forming intermolecular complexes. We used two different techniques to exclude the formation of intermolecular complexes. First, nondenaturing electrophoresis of the oligonucleotides showed that in the presence of 50 mM KCl or 100 mM NaCl over 90% of the material was present as a single band in each case (Supporting Information, Figure 1). Previous studies in which there was equilibrium between inter- and intramolecular complexes showed the presence of several bands with different mobilities (*26*). A small amount (approximately 5%) of the material was evident as a band of lower mobility with oligonucleotides G3H2 and G3T, suggesting that these oligonucleotides may be able to form intermolecular complexes. However, these experiments were performed with much higher oligonucleotide concentrations (7.5 $\mu$M) than those used in the fluorescence melting experiments. Second, the $T_m$ of an intramolecular complex should be independent of concentration, in contrast to an intermolecular complex for which the $T_m$ should increase with oligonucleotide concentration. We therefore compared the melting and annealing curves for all of the oligonucleotides used in this work at 0.1 and 1.0 $\mu$M (Supporting Information, Figure 2). In almost all cases the $T_m$ values differed by less than 0.5 K at the two concentrations. The only exceptions were with G4T2 and myc-1, for which the two $T_m$ values differed by 1.5 K.

*Annealing Curves for Intramolecular Quadruplexes*. Fluorescence annealing curves were determined for all of the oligonucleotides under a range of ionic conditions. Figure 3 shows representative annealing curves obtained in 10 mM buffers, while all of the $T_m$ and $\Delta H$ values are summarized

Table 2: Thermodynamic Parameters Derived from the Fluorescence Annealing Curves

| | $K^+$ | | | $Na^+$ | | |
|---|---|---|---|---|---|---|
| oligo | $[M^+]$ (mM) | $T_m$ (K) | $\Delta H_{app}$[a] (kJ·mol$^{-1}$) | $[M^+]$ (mM) | $T_m$ (K) | $\Delta H$ (kJ·mol$^{-1}$) |
| G3TTA | 5 | 318.3 | −172 | 5 | 301.3 | −94 |
| | 10 | 324.2 | −188 | 10 | 310.8 | −139 |
| | 20 | 331.9 | −215 | 20 | 318.5 | −175 |
| | 30 | 339.6 | −244 | 40 | 325.6 | −192 |
| | 40 | 342.2 | −254 | 50 | 329.3 | −198 |
| | 50 | 346.3 | −261 | 75 | 333.8 | −209 |
| | 75 | 348.9 | −268 | 100 | 335.9 | −215 |
| | 100 | 354.9 | −277 | 200 | 343.2 | −233 |
| G3H2 | 5 | 300.5 | −82 | 5 | too unstable | |
| | 10 | 314.1 | −124 | 10 | too unstable | |
| | 20 | 326.6 | −164 | 20 | 297.2 | −113 |
| | 30 | 338.9 | −232 | 40 | 309.6 | −154 |
| | 40 | 342.3 | −252 | 50 | 313.8 | −161 |
| | 50 | 347.6 | −283 | 75 | 318.8 | −168 |
| | 75 | 351.0 | −294 | 100 | 322.5 | −166 |
| | 100 | 358.0 | −310 | 200 | 330.4 | −186 |
| G3AT | 1 | 312.1 | −61 | 10 | 311.8 | −84 |
| | 5 | 321.2 | −115 | 20 | 311.2 | −89 |
| | 10 | 328.8 | −134 | 40 | 315.9 | −90 |
| G3T | 1 | too stable | | 10 | 359.3 | −219 |
| | 5 | too stable | | 20 | too stable | |
| G3T2 | 1 | 353.1 | −239 | 10 | 333.4 | −169 |
| | 5 | 360.1 | −287 | 20 | 336.5 | −188 |
| | 10 | too stable | | 40 | 340.9 | −189 |
| G4T2 | 1 | 339.4 | −133 | 10 | 325.0 | −172 |
| | 5 | 344.8 | −168 | 20 | 330.8 | −191 |
| | 10 | 352.2 | −187 | 40 | 337.9 | −204 |
| G3A3 | 10 | too unstable | | 40 | too unstable | |
| myc-1 | 1 | 348.0 | −145 | 10 | 327.1 | −137 |
| | 5 | 357.5 | −189 | 20 | 332.6 | −162 |
| myc-2 | 10 | too stable | | 40 | 339.1 | −178 |
| | 1 | too stable | | 10 | 333.1 | −129 |
| | 5 | too stable | | 20 | 337.7 | −136 |
| | 10 | too stable | | 40 | 342.7 | −141 |

[a] In the presence of low concentrations of potassium (<50 mM) there is often hysteresis between the melting and annealing curves. The values presented are apparent $\Delta H$ values calculated from the annealing phases.

in Table 2. As expected, all of the complexes are more stable in potassium-containing than sodium-containing buffers.

Looking first at the data for G3TTA, the human telomere repeat sequence, it can be seen that the $T_m$ values are between 10 and 15 K higher in potassium-containing than sodium-containing buffers, and the $\Delta H$ values differ by between 40 and 60 kJ·mol$^{-1}$. The $\Delta H$ values also show a strong dependence on the ionic strength. This is an unusual observation since simple polyelectrolyte theory suggests that there should be no change in enthalpy with salt concentration. However, this has been observed in other studies with quadruplexes and is consistent with the presence of specific ion binding sites in the folded structure (*24*).

For oligonucleotide G3H2 the TTA loops are replaced with two hexaethylene glycol linkers. This oligonucleotide produces melting profiles similar to those of G3TTA, showing that the bases in the loops are not essential for quadruplex formation. However, the $T_m$ values are about 15 K lower than for G3TTA (except at high potassium concentrations), and the $\Delta H$ values are lower by 50−60 kJ·mol$^{-1}$. The $T_m$ and $\Delta H$ values for this structure are very dependent on the potassium concentration, and it is more stable than G3TTA at elevated potassium concentrations.

Oligonucleotide G3T, in which the TTA loops are replaced with a single T residue, produces a very stable complex, which melts at about 359 K in the presence of 10 mM sodium. This oligonucleotide is similar to sequence T30695 (*15*, *16*, *24*), which has been shown to adopt a structure containing two stacked G-quartets linked by TG bases in the loops. At higher sodium concentrations or in the presence of potassium the complex does not melt within the accessible temperature range. It should be noted that previous melting studies with T30695 (*15*, *16*, *24*) have been performed in the presence of 20 mM $Li^+$ to reduce the stability. The low fluorescence of these structures suggests that the fluorophore and quencher are in close proximity and that the oligonucleotide has adopted a folded structure. Addition of a second thymidine, generating oligonucleotide G3T2, produces a structure with a stability that is intermediate to G3TTA and G3T. Although the melting curve has the usual shape in the presence of sodium, a biphasic curve is evident with potassium, suggesting that this may adopt multiple structural forms with different stabilities. Addition of a further guanine (oligonucleotide G4T2) reduces the melting temperature, and a simple transition is observed in the presence of potassium. This structure has a higher $T_m$ than G3TTA though the $\Delta H$ values are very similar. Replacing the TTA loops with AAA (oligonucleotide G3A3) generates a structure with a very different melting profile in which most of the transition occurs below 300 K. Oligonucleotide G3AT is similar to G3A3, but the second and third loops are replaced by TTT. This modification increases the melting temperatures so that the $T_m$ values are comparable to G3TTA, though the $\Delta H$ values are much lower. This structure is less stable than G3TTA in the presence of sodium but is slightly more stable in the presence of potassium.

Oligonucleotides myc-1 and myc-2 were designed to resemble portions of the G-rich sequence of the *c-myc* promoter ($G_4AG_3TG_4AG_3TG_4AAGG$), which has been shown to adopt a G-quadruplex structure (*25*, *26*, *35*). Both of these oligonucleotides show melting profiles that are consistent with the formation of stable quadruplexes. Myc-1 ($G_4AG_4TG_4AG_4T$) melts at a lower temperature than myc-2 ($G_4AG_3TG_4AG_3T$), even though it contains one less guanine residue in the repeating unit. Both of these oligonucleotides melt at very high temperatures in the presence of potassium. Indeed, in potassium-containing buffers, there is almost no detectable melting of myc-2 at the highest temperatures accessible in this system.

*Relative Stability of Quadruplexes and Duplexes*. Within the cell most G-rich sequences with the potential to adopt G-quadruplexes will be present along with their complementary C-rich strands, which will generate competing duplex structures. The formation of quadruplex or duplex structures will depend on their relative stability. We have used these fluorescence melting experiments to assess the relative stability of Watson−Crick duplexes and intramolecular quadruplexes formed by these oligonucleotides. The principle of this assay is shown in Figure 1B. When the G-rich oligonucleotide binds to its complementary C-rich sequence, the fluorophore and quencher are separated by a large distance, at opposite ends of the DNA duplex. This will produce a large fluorescence signal. Since the duplex is more rigid than the random coil, the time-averaged distance between the fluorophore and quencher will be greater in the duplex form, resulting in a larger fluorescence signal. The relative order of the fluorescence signals for the different

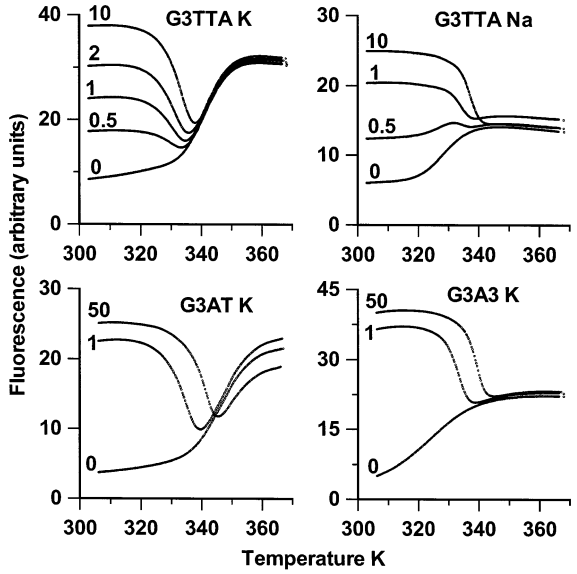


FIGURE 4: Fluorescence annealing curves for the intramolecular quadruplexes formed by G3TTA, G3AT, and G3A3 in the absence and presence of the complementary oligonucleotides. The quadruplex-forming oligonucleotides were all at a concentration of 0.25 $\mu$M. The numbers beside each curve show the fold excess of the complementary oligonucleotide. 0 shows the melting curve in the absence of added complement. These curves were obtained in 50 mM potassium phosphate, pH 7.4, or 50 mM sodium phosphate, pH 7.4.

species will therefore be duplex > single strand ≫ quadruplex. Representative annealing curves for the each of the fluorescently labeled oligonucleotides in the presence of different amounts of their complementary C-rich strands are shown in Figures 4−6.

The upper panels of Figure 4 show the annealing profiles for the human telomeric sequence G3TTA in the presence of potassium or sodium on addition of the complementary C-rich oligonucleotide. It can be seen that, in the presence of potassium and a 10-fold excess of the complementary strand, the fluorescence is highest at low temperatures, consistent with the formation of a Watson−Crick duplex. As expected, this fluorescence is greater than that of the fully melted (random coil) form which predominates at temperatures above 355 K. The remainder of the fluorescence profile is unusual but is explained by competition between the duplex and quadruplex forms. As the temperature is decreased, the fluorescence profile initially follows the annealing curve for the quadruplex alone. However, at around 340 K there is a large increase in fluorescence, which corresponds to duplex formation. This transition moves to higher temperatures in the presence of increasing concentrations of the C-rich oligonucleotide, as expected for an intermolecular reaction (in contrast to quadruplex formation which is an intramolecular process). These results suggest that the quadruplex form predominates at elevated temperatures, while the duplex is more stable at temperatures below 340 K. Addition of an equimolar amount of the C-rich oligonucleotide does not produce the full increase in fluorescence at low temperatures, suggesting that some quadruplex is still present. However, it should be noted that since the formation and dissociation of these structures are slow processes, these curves may not be at thermodynamic equilibrium. The profiles in the presence of sodium (upper

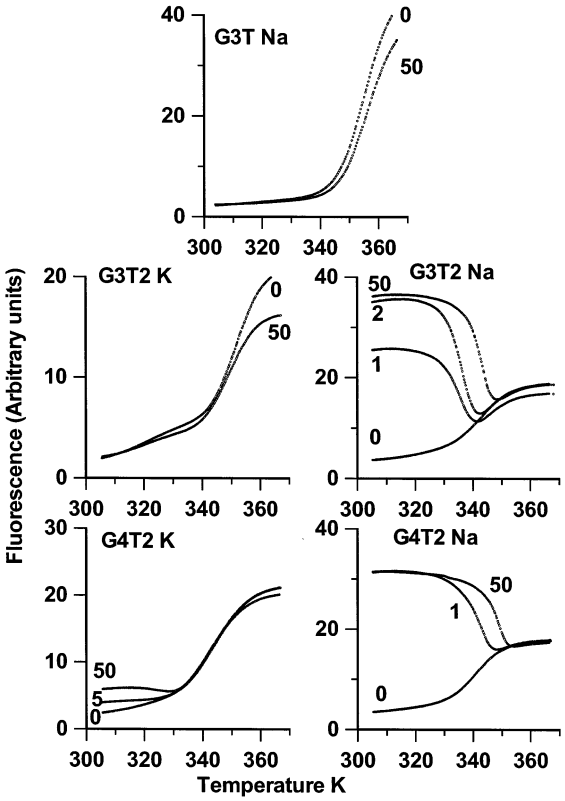


FIGURE 5: Fluorescence annealing curves for the intramolecular quadruplexes formed by G3T, G3T2, and G4T2 in the absence and presence of the complementary oligonucleotides. The quadruplex-forming oligonucleotides were all at a concentration of 0.25 $\mu$M. The numbers beside each curve show the fold excess of the complementary oligonucleotide. 0 shows the melting curve in the absence of added complement. These curves were determined in the following buffers: G3T Na, 1 mM sodium phosphate, pH 7.4; G3T2 K, 1 mM potassium phosphate, pH 7.4; G3T2 Na, 20 mM sodium phosphate, pH 7.4; G4T2 K, 5 mM potassium phosphate, pH 7.4; G4T2 Na, 20 mM sodium phosphate, pH 7.4.

right panel) show a simple increase in fluorescence on lowering the temperature, corresponding to the transition from random coil to duplex. This suggests that under these conditions the intermolecular duplex is formed in preference to the intramolecular quadruplex.

Similar experiments could not be performed with oligonucleotide G3H2 as the hexaethylene glycol linkers prevent the formation of a stable duplex under any conditions and addition of C-rich oligonucleotides had no effect on the melting of this oligonucleotide (not shown).

Oligonucleotides G3A3 and G3AT do not form a stable quadruplex in the presence of sodium and show a simple increase in fluorescence on annealing with the complementary oligonucleotide (not shown), corresponding to the single strand to duplex transition. The results of experiments with these oligonucleotides in the presence of 50 mM potassium are shown in the lower panels of Figure 4. When G3AT is cooled in the presence of the complementary oligonucleotide, the fluorescence profiles first follow the annealing curve for the quadruplex alone. However, at temperatures below about 345 K the fluorescence increases, consistent with the formation of a duplex structure. Unlike G3TTA this fluorescence reversal is almost completed by addition of an equimolar amount of the C-rich oligonucleotide. Addition of a 50-fold excess of the complement increases the

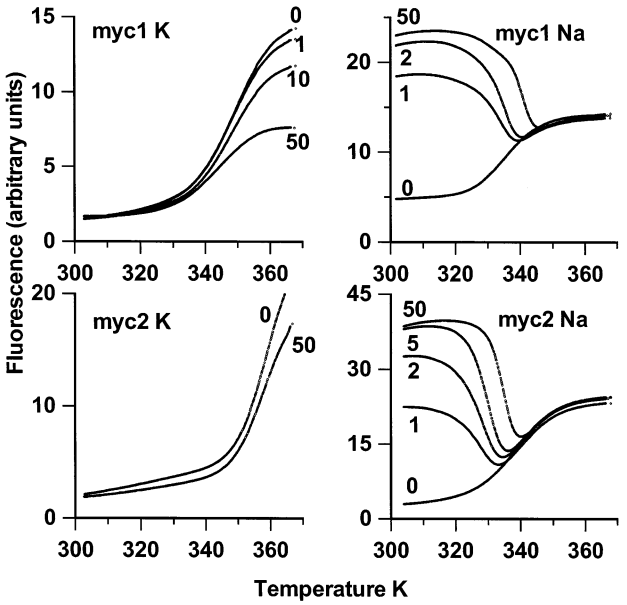


FIGURE 6: Fluorescence annealing curves for the intramolecular quadruplexes formed by myc-1 and myc-2 in the absence and presence of the complementary oligonucleotides. The quadruplex-forming oligonucleotides were all at a concentration of 0.25 $\mu$M. The numbers beside each curve show the fold excess of the complementary oligonucleotide. 0 shows the melting curve in the absence of added complement. These curves were obtained in 1 mM potassium phosphate, pH 7.4, or 10 mM sodium phosphate, pH 7.4.

temperature of the lower transition as expected for an intermolecular reaction and has little effect on the quadruplex transition. A similar effect is seen with oligonucleotide G3A3 except that addition of the C-rich oligonucleotide completely abolishes quadruplex formation and there is a simple increase in fluorescence on cooling corresponding to a single strand to quadruplex transition.

Figure 5 shows the annealing profiles for oligonucleotides G3T, G3T2, and G4T2. In the presence of potassium G3T forms a very stable structure, which melts at temperatures above 370 K. In the presence of low concentrations of sodium the melting profile is within the accessible temperature range, and this is not affected by addition of the C-rich complement. Even when the complement is added at 50-fold excess, there is no evidence for the formation of a duplex. A similar effect is seen with G3T2 and G4T2 in the presence of potassium, though the profiles for the latter suggest that a small amount of duplex may be present at low temperatures. In contrast, the annealing profiles for these oligonucleotides in the presence of sodium reveal that the intermolecular duplexes are formed in preference to the intramolecular quadruplexes. There is an initial decrease in the fluorescence of G3T2 as this is cooled, suggesting that the quadruplex begins to form, but this is rapidly replaced by an increase, which is characteristic of duplex formation. G4T2 shows no evidence for quadruplex formation in the presence of the competing oligonucleotide.

Figure 6 shows similar annealing profiles for the two oligonucleotides that are related to a portion of the *c-myc* promoter sequence. In the presence of potassium there is no evidence for duplex formation; the low fluorescence at low temperatures suggests that the intramolecular quadruplex is more stable than the competing intermolecular duplex. The fluorescence profiles for these oligonucleotides are very different in the presence of sodium and show clear evidence for duplex formation. Equimolar concentrations of the complementary oligonucleotides do not give the full increase in fluorescence signal at low temperatures, suggesting that some quadruplex structures may be retained (especially with myc-2).

## DISCUSSION

*Quadruplex−Duplex Equilibrium*. Several of the oligonucleotides used in this study are related to naturally occurring G-rich sequences that have been implicated in quadruplex formation; G3TTA is the human telomeric repeat and G4T2 is the *Tetrahymena* repeat, while myc-1 and myc-2 are related to portions of the *c-myc* promoter sequence. Although the ends of chromosomes may be single stranded, in every other genomic location quadruplex formation will be in competition with the duplex that is formed by interaction with the complementary C-rich strand. If quadruplex formation is biologically relevant, then in some circumstances it must be favored over duplex formation, though this may be facilitated by the interaction with specific proteins. The present results show that, within the kinetic constraints of these experiments, quadruplex formation predominates for G4T2, myc-1, and myc-2 in the presence of potassium (the physiologically relevant intracellular cation). With G3TTA there appears to be a mixture of quadruplex and duplex forms at physiological temperatures. These results therefore demonstrate that it is possible to form these higher order DNA structures, even in the presence of the complementary strand. This conversion has previously been facilitated by interaction of a quadruplex-binding ligand with the *c-myc* promoter sequence (*26*). The situation in genomic DNA will be more biased toward duplex formation, as the opposite strand will be kept in close proximity; however, this has the potential to fold into structures related to the i-motif.

*Interaction with Metal Ions*. Many studies have shown that DNA quadruplexes are selectively stabilized by potassium, and this is confirmed by the present studies. The preference for potassium over sodium may reflect differences in its interaction with the stacked G-quartets, differences in energies of solvation, or the formation of different quadruplex folds. Indeed, structural studies have suggested that the human telomeric sequence folds into an antiparallel arrangement in the presence of sodium (*12*) but a parallel structure in potassium (*13*). Differences in structure are also suggested by the present results, for which the thermodynamic parameters for all the quadruplexes are more sensitive to potassium than sodium concentration. The hysteresis observed in the melting and annealing profiles at concentrations of potassium (but not sodium) also indicates differences in the interaction with these ions and is consistent with the suggestion that formation of the final stable complex involves a very slow reaction step. The properties of G3H2 are particularly unusual as it is less stable than G3TTA at low potassium concentrations but is more stable at elevated potassium. It is possible that the presence of the two hexaethylene glycol linkers (each 18 atoms long) allows this sequence to fold in a completely parallel fashion, as usually observed for intermolecular complexes formed with four G-containing strands (*5*, *6*). In contrast, although crystal structures have shown that G3TTA

can fold with the G-strands in a parallel orientation (*13*), the solution structures have also shown an antiparallel strand arrangement (*12*).

*Different Quadruplex Structures*. One surprising observation is that quadruplex stability is not necessarily improved by increasing the length of the G-tracts or the linking bases. For example, G3T2 is more stable than G4T2, and G3T is the most stable structure that we have investigated. Similarly, myc-2 is more stable than myc-1 even though it contains one less guanine in the repeating unit. These observations are consistent with several quadruplex structures, which show that the number of stacked G-quartets is not necessarily the same as the number of contiguous guanines. For example, G4T2 (*11*) and G3T (*15*) form structures that contain three and two stacked G-quartets, respectively, though in principle they could generate four and three; in contrast, G3TTA forms structures that contain three guanine quartets (*12*, *13*). The conformational details are therefore dependent on the length and base composition of the looped bases, in a way that is presently poorly understood. In the presence of potassium G3T2 displays a biphasic melting curve, which presumably indicates the presence of more than one stable quadruplex structure. A similar effect is seen with the complete G-rich sequence of the *c-myc* promoter ($G_4AG_3TG_4AG_3TG_4AAGG$) which can adopt several stable conformations. Recent studies have shown that the chair form, which stacks in a similar way to the shorter sequences used in the present studies, is the biologically relevant form (*26*).

## SUPPORTING INFORMATION AVAILABLE

Two figures showing the mobility of different DNA fragments and representative melting profiles for several oligonucleotides. This material is available free of charge via the Internet at http://pubs.acs.org.

## REFERENCES


1. Gellert, M., Lipsett, M. N., and Davies, D. R. (1962) Helix formation by guanylic acid, *Proc. Natl. Acad. Sci. U.S.A. 48*, 2013−2018.
2. Williamson, J. R. (1993) Guanine quartets, *Curr. Opin. Struct. Biol. 3*, 357−362.
3. Keniry, M. A. (2000) Quadruplex structures in nucleic acids, *Biopolymers 56*, 123−146.
4. Simonsson, T. (2001) G-quadruplex DNA structures−variations on a theme, *Biol. Chem. 382*, 621−628.
5. Laughlan, G., Murchie, A. I. H., Norman, D. G., Moore, M. H., Moody, P. C., Lilley, D. M. J., and Luisi, B. (1994) The high-resolution crystal structure of a parallel stranded guanine tetraplex, *Science 265*, 520−524.
6. Phillips, K., Dauter, Z., Murchie, A. I., Lilley, D. M. J., and Luisi, B. (1997) The crystal structure of a parallel-stranded guanine tetraplex at 0.95 Angstrom resolution, *J. Mol. Biol. 273*, 171−182.
7. Sundquist, W. I., and Klug, A. (1989) Telomeric DNA dimerizes by formation of guanine tetrads between hairpin loops, *Nature 342*, 825−829.
8. Keniry, M. A., Strahan, G. D., Owen, E. A., and Shafer, R. H. (1995) Solution structure of the $Na^+$ form of the dimeric guanine tetraplex $[d(G_3T_4G_3]_2$, *Eur. J. Biochem. 233*, 631−643.
9. Haider, S., Parkinson, G. N., and Neidle, S. (2002) Crystal structure of the potassium form of the *Oxytricha nova* G-quadruplex, *J. Mol. Biol. 320*, 189−200.
10. Wang, Y., and Patel, D. J. (1995) Solution structure of the *Oxytricha* telomeric repeat $d[G_4(T_4G_4)_3]$, *J. Mol. Biol. 251*, 76−94.
11. Wang, Y., and Patel, D. J. (1994) Solution structure of the *Tetrahymena* telomeric repeat $d(T_2G_4)_4$ G-tetraplex, *Structure 2*, 1141−1156.
12. Wang, Y., and Patel, D. J. (1993) Solution structure of the human telomeric repeat $d[AG_3(T_2AG_3)_3]$ G-tetraplex, *Structure 1*, 263−282.
13. Parkinson, G. N., Lee, M. P. H., and Neidle, S. (2002) Crystal structure of parallel quadruplexes from human telomeric DNA, *Nature 417*, 876−880.
14. Schultze, P., Macaya, R. F., and Feigon, J. (1994) Three-dimensional solution structure of the thrombin-binding DNA aptamer d(GGTTGGTGTGGTTGG), *J. Mol. Biol. 234*, 1532−1547.
15. Jing, N., and Hogan, M. E. (1998) Structure−activity of tetrad-forming oligonucleotides as a potential anti-HIV therapeutic drug, *J. Biol. Chem. 273*, 34992−34999.
16. Jing, N., Marchand, C., Liu, J., Mitra, R., Hogan, M. E., and Pommier, Y. (2000) Mechanism of inhibition of HIV-1 integrase by G-tetrad forming oligonucleotides in vitro, *J. Biol. Chem. 275*, 21460−21467.
17. Smirnov, I., and Shafer, R. H. (2000) Effect of loop sequence and size on DNA aptamer stability, *Biochemistry 39*, 1462−1468.
18. Williamson, J. R., Raghuraman, M. K., and Cech, T. R. (1989) Mono-valent cation induced structure of telomeric DNA−The G-quartet model, *Cell 59*, 871−880.
19. Sen, D., and Gilbert, W. (1990) A sodium−potassium switch in the formation of 4-stranded G4-DNA, *Nature 344*, 410−414.
20. Deng, H., and Braunlin, W. H. (1996) Kinetics of sodium ion binding to DNA quadruplexes, *J. Mol. Biol. 255*, 476−483.
21. Miura, T., Benevides, J. M., and Thomas, G. J., Jr. (1995) A phase-diagram for sodium and potassium-ion control of polymorphism in telomeric DNA, *J. Mol. Biol. 248*, 233−238.
22. Sen, D., and Gilbert, W. (1992) Guanine quartet structures, *Methods Enzymol. 211*, 191−199.
23. Hud, N. V., Smith, F. W., Anet, F. A., and Feigon, J. (1996) The selectivity for $K^+$ versus $Na^+$ in DNA quadruplexes is dominated by relative free energies of hydration−a thermodynamic analysis by H-1 NMR, *Biochemistry 35*, 15383−15390.
24. Jing, N., Rando, R. F., Pommier, Y., and Hogan, M. E. (1997) Ion selective folding of loop domains in a potent anti-HIV oligonucleotide, *Biochemistry 36*, 12498−12505.
25. Simmonsson, T., Pecinka, P., and Kubista, M. (1998) DNA tetraplex formation in the control region of c-myc, *Nucleic Acids Res. 26*, 1167−1172.
26. Rangan, A., Fedoroff, O. Y., and Hurley, L. H. (2001) Induction of duplex to G-quadruplex transition in the c-*myc* promoter region by a small molecule, *J. Biol. Chem. 276*, 4640−4646.
27. Sen, D., and Gilbert, W. (1988) Formation of parallel 4-stranded complexes by guanine-rich motifs in DNA and its implications for meiosis, *Nature 334*, 364−366.
28. Catasti, P., Chen, X., Moyzis, R. K., Bradbury, E. M., and Gupta, G. (1996) Structure−function correlations of the insulin-linked polymorphic region, *J. Mol. Biol. 264*, 534−545.
29. Schultze, P., Macaya, R. F., and Feigon, J. (1993) Thrombin-binding DNA aptamer forms a unimolecular quadruplex structure in solution, *J. Mol. Biol. 235*, 1532−1547.
30. Miura, T., and Thomas, G. J., Jr. (1995) Structure and thermodynamics of interstrand guanine association in quadruplex telomeric DNA, *Biochemistry 34*, 9645−9654.
31. Hardin, C. C., Watson, T., Corregan, M., and Bailey, C. (1992) Cation-dependent transition between the quadruplex and Watson−Crick hairpin forms of $d(CGCG_3GCG)$, *Biochemistry 31*, 833−841.
32. Wyatt, J. R., Davis, P. W., and Freier, S. M. (1996) Kinetics of G-quartet mediated tetramer formation, *Biochemistry 35*, 8002−8008.
33. Phan, A. T., and Mergny, J.-L. (2002) Human telomeric DNA: G-quadruplex, i-motif and Watson−Crick double helix, *Nucleic Acids Res. 30*, 4618−4625.
34. Li, W., Wu, P., Ohmichi, T., and Sugimoto, N. (2002) Characterization and thermodynamic properties of quadruplex/duplex competition, *FEBS Lett. 526*, 77−81.
35. Darby, R. A. J., Sollogoub, M., McKeen, C., Brown, L., Risitano, A., Brown, L., Barton, C., Brown, T., and Fox, K. R. (2002) High throughput measurement of duplex, triplex and quadruplex melting curves using molecular beacons and a Light Cycler, *Nucleic Acids Res. 30*, e39.


BI026997V